Two-dimensional solitons in PT linear lattice potentials

Jianhua Zeng* and Yueheng Lan

State Key Laboratory of Low Dimensional Quantum Physics, Department of Physics, Tsinghua University, Beijing 100084, China

(Received 6 December 2011; published 17 April 2012)

We investigate two-dimensional (2D) ordinary and gap solitons in the 2D and the quasi-one-dimensional parity-time ($\mathcal{PT}$) linear lattice potentials. The stability diagrams for both versions of $\mathcal{PT}$ potentials are given. Particularly, we find that 2D gap solitons with self-attractive nonlinearity may exist in the $\mathcal{PT}$ lattice, but they are unstable due to the collapse instability.

DOI: 10.1103/PhysRevE.85.047601 PACS number(s): 05.45.Yv, 11.30.Er, 03.75.Lm, 42.65.Tg

I. INTRODUCTION

Over a decade ago, Bender and Boettcher reported [1] that spectra can be entirely real in a wide class of non-Hermitian Hamiltonians if the system is parity-time ($\mathcal{PT}$) symmetric. Since then, considerable attention has been focused on this subject. The $\mathcal{PT}$ symmetry requires that the real part of the $\mathcal{PT}$ complex potential is an even function of position while the imaginary part is odd. Interestingly, $\mathcal{PT}$ Hamiltonians can be recognized as a general class of pseudo-Hermitian systems given that their eigenenergies are real. Probably the most intriguing property in a $\mathcal{PT}$ Hamiltonian system is the existence of an "exceptional point" (critical threshold), below which the spectrum is real, while above which the system undergoes a rather sudden "$\mathcal{PT}$-symmetry-breaking" phase transition with the spectrum becoming complex. The characteristics of this "exceptional point" or $\mathcal{PT}$-symmetry breaking are extensively addressed in many different contexts [2–11].

It is suggested [12,13] that optics offers a highly fertile ground for experimental realization and detailed investigation of systems with $\mathcal{PT}$ symmetry, provided that a medium is created with alternating regions of gain and loss. Pioneering theoretical works [14–16] stimulated recent experimental studies that eventually resulted in the observation of the $\mathcal{PT}$-symmetry breaking in both passive [17] and active [18] optically coupled systems. This will probably enable manufacturing of integrated $\mathcal{PT}$ photonic devices with extraordinary capability, such as double-refraction or energy flow tailoring. A new direction concerning $\mathcal{PT}$ optical lattices [19,20] and the related $\mathcal{PT}$-based solitons can also be envisaged. Hence, further exploration of general properties of solitons in various $\mathcal{PT}$ potentials is recalled. The existence, stability, and propagation dynamics of the one-dimensional (1D) optical solitons in a $\mathcal{PT}$ linear periodic potential have been examined in detail in Ref. [13]. The 1D solitons supported by the $\mathcal{PT}$-symmetric nonlinear lattices were also reported recently [21,22]. In order to achieve an insight into the formation of $\mathcal{PT}$-based solitons [13,21,22], the current paper studies how a soliton is created and stabilized in a two-dimensional (2D) space.

In this paper, we investigate disparate types of 2D solitons (both ordinary and gap ones) in a full 2D $\mathcal{PT}$ linear lattice potential $\{V(x,y) = 4(\cos^2 x + \cos^2 y) + 4iV_0[\sin(2x) + \sin(2y)]\}$and a quasi-1D (Q1D) [i.e., $V(x) = 4\cos^2 x + 4iV_0 \sin(2x)$] one. It is relevant to stress that our model is substantially different from those obtained recently in the $\mathcal{PT}$ waveguide study, where the 2D optical gap solitons have not yet been investigated [13]. We reveal that the imaginary part of the solitons always emerges in the form of a dipole. It is also found that, in contrast to those reported [13,19,20] in the 1D case, the stable 2D solitons can only exist for small V_0. They become less stable with increasing V_0. Thus, we come to the conclusion that the 2D solitons survive only for sufficiently small V_0. An open question on 2D gap solitons under self-attractive intrinsic nonlinearity is also tested in the $\mathcal{PT}$ model; our study shows that such gap solitons exist under certain conditions, and they are unstable. All the results reported here are based on direct numerical simulations, as the analytical computation would be too cumbersome.

The rest of the article is organized as follows. The model and its band spectrum are introduced in Sec. II. Localized states in the semi-infinite gap and the first and second band gaps are reported in Sec. III. The 2D gap soliton with self-attractive nonlinearity and the localized states in the low-dimensional $\mathcal{PT}$ potential are explored separately in Secs. IV and V, and the article is concluded in Sec. VI.

II. THE MODEL AND ITS BAND SPECTRUM

The system with the 2D $\mathcal{PT}$ linear lattice potential can be described with the scaled Gross-Pitaevskii [23] (or nonlinear Schrödinger) equation for the Bose-Einstein condensation wave function (or the amplitude of the electromagnetic wave in optics), $\psi(x,y,t)$:

$$i\psi_t = -(1/2)\left(\partial_x^2 + \partial_y^2\right)\psi - V(x,y)\psi - g|\psi|^2\psi, \quad (1)$$

where t is the time coordinate (or the propagation distance in optics) and the nonlinear coupling is normalized such that $g \equiv \pm 1$, with the plus and the minus sign corresponding to the self-attractive and the self-repulsive nonlinearity, respectively. As mentioned above, the $\mathcal{PT}$ potential is then to be $V(x,y) = 4(\cos^2 x + \cos^2 y) + 4iV_0[\sin(2x) + \sin(2y)]$.

Stationary solutions to Eq. (1) with chemical potential μ (or the propagation constant $-\mu$ in optics) are in the form of $\psi(x,y,t) = \phi(x,y)\exp(-i\mu t)$, where the function $\phi(x,y)$ satisfies

$$\mu\phi = -(1/2)\left(\partial_x^2 + \partial_y^2\right)\phi - V(x,y)\phi - g|\phi|^2\phi. \quad (2)$$

The band spectrum of Eq. (1) in the 2D $\mathcal{PT}$ linear lattice potential can be computed with a linearization of Eq. (2)

*zengjianhua1981@gmail.com

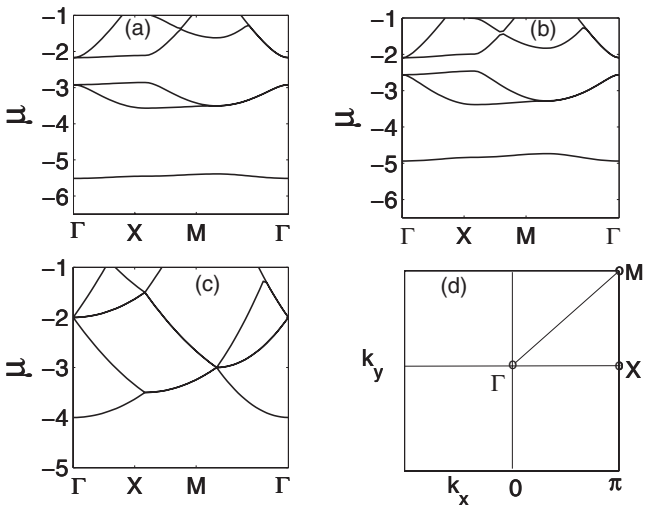

FIG. 1. The band spectrum of the linearization of Eq. (2) in the irreducible zone (triangle ΓXM) of the first Brillouin zone for the $\mathcal{PT}$ linear lattice potential $V(x,y) = 4(\cos^2 x + \cos^2 y) + 4i\,V_0[\sin(2x) + \sin(2y)]$ at (a) $V_0 = 0.02$, (b) $V_0 = 0.33$, and (c) $V_0 = 0.5$. (d) shows the first Brillouin zone of the $\mathcal{PT}$ lattice in the reciprocal lattice space; the high-symmetry points (ΓXM) in the irreducible zone are marked.

in a way similar to that in solid-state physics. Specifically, according to the Bloch theorem, the $\mathcal{PT}$ lattice is first mapped onto the reciprocal lattice space, and then the band structure is obtained along the directions with the highest symmetries of the irreducible zone (triangle ΓXM) in the first Brillouin zone [see Fig. 1(d)]. In Fig. 1 we show the associated spectrum for $V_0 = 0.02$ (a), $V_0 = 0.33$ (b), and $V_0 = 0.5$ (c). As usual, there exists a semi-infinite gap (semi-infinite region below the first band), together with gaps with different orders—including the first and the second order when $V_0 < 0.5$. The $\mathcal{PT}$-symmetry breaking happens right at the phase transition point $V_0 = 0.5$. Above this value the first and the second band gaps will merge and the band gap disappears [Fig. 1(c)], in analogy to what is reported previously [12,13]. In the following, we will construct localized stationary modes of Eq. (2) and then test their stability with numerical simulations by adding small random perturbations to the so-found solutions and integrating Eq. (1).

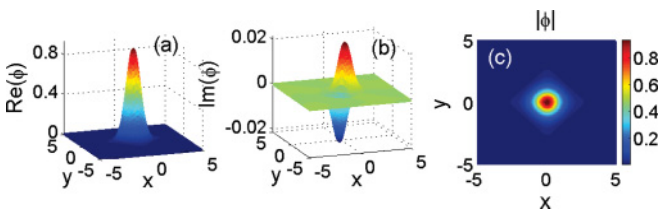

FIG. 2. (Color online) A typical example of a stable ordinary soliton of the model with the full 2D $\mathcal{PT}$ linear potential, for $V_0 = 0.02$, $g = +1$, $\mu = -5.85$, and $N = 0.94$. (a) and (b) are the real and imaginary parts of wave function $\phi(x,y)$; (c) is the contour plot of mod $|\phi|$.

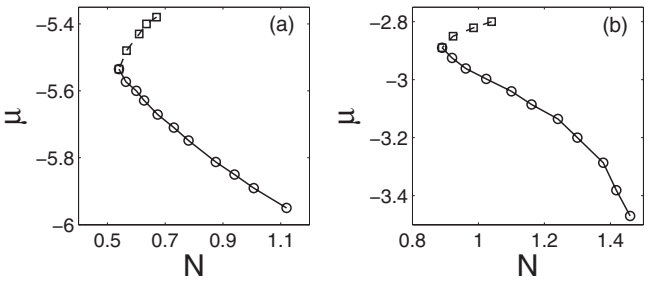

FIG. 3. The bifurcation diagram $\mu(N)$ for the stable (solid curve) and unstable (dashed curve) ordinary solitons (in the semi-infinite gap) of the model Eq. (2) at $V_0 = 0.02$ with (a) the 2D $\mathcal{PT}$ linear potential and (b) the Q1D potential.

III. LOCALIZED STATES IN THE SEMI-INFINITE GAP AND THE FIRST AND SECOND BAND GAPS

To construct the localized state, we use the Gaussian ansatz as the input, $\phi(x,y) = A\exp[-(x^2+y^2)/(2W^2)]$, with amplitude A and width W. Based on the fact that the real and the imaginary component of the $\mathcal{PT}$ potential are even and odd, respectively, we may define the norm $N = \int_{-\infty}^{+\infty}\int_{-\infty}^{+\infty}\phi(x,y)\phi^*(-x,-y)dxdy$ instead of the commonly used $N = \int_{-\infty}^{+\infty}\int_{-\infty}^{+\infty}|\phi(x,y)|^2dxdy$ [12].

A stable ordinary soliton, generated in the semi-infinite gap with self-attractive nonlinearity, is shown in Fig. 2. We can see that the real part of the soliton is similar to the usual quasi-isotropic localized state, while the imaginary part is in a dipole mode. A bifurcation diagram for soliton stability is depicted in Fig. 3(a). A saddle-node bifurcation occurs at $N \approx 0.53$ where a stable and an unstable branch of solitons are generated. The curve $\mu(N)$ for the stable solitons obeys the Vakhitov-Kolokolov (VK) criterion [24], $\partial\mu/\partial N < 0$, while the branch $\partial\mu/\partial N > 0$ corresponds to unstable solitons, similar to those found in both the 1D [25] and the 2D [26] incommensurate linear and nonlinear lattices. The unstable solitons will decay into radiating waves (i.e., in Fig. 4) under very small perturbation.

Compared with ordinary solitons, gap solitons have more complex profiles, i.e., usually with multiple side peaks. Examples of stable gap solitons, generated in both the first and the second band gap with self-repulsive nonlinearity, are displayed in Figs. 5 and 6, respectively. More and higher side peaks appear in Fig. 6, since solitons in the second band gap have larger energies than those in the first band gap. As shown

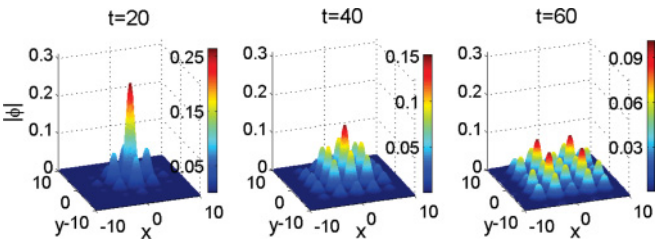

FIG. 4. (Color online) The evolution of an unstable ordinary soliton of Eq. (1) with the 2D $\mathcal{PT}$ linear potential, for $V_0 = 0.02$, $g = +1$, $\mu = -5.43$, and $N = 0.42$. Initial perturbation is 1% in size of the soliton amplitude or phase.

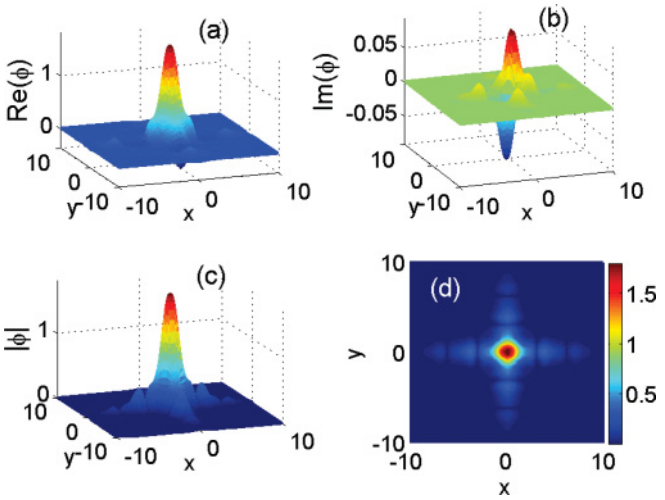

FIG. 5. (Color online) A typical example of a stable gap soliton in the first band gap with the full 2D $\mathcal{PT}$ linear potential, for $V_0 = 0.02$, $g = -1$, $\mu = -3.6$, and $N = 3.5$. (a) and (b) are the real and imaginary parts of wave function $\phi(x,y)$, (c) is the mod $|\phi|$, and (d) is its contour plot.

in Fig. 7, unlike the ordinary soliton, the stable gap soliton always features $\partial\mu/\partial N > 0$, satisfying the "anti-Vakhitov-Kolokolov" criterion [25,26]. Like the ordinary soliton, the unstable gap soliton also suffers decay.

IV. EXISTENCE OF THE 2D GAP SOLITON WITH SELF-ATTRACTIVE NONLINEARITY

Let us consider here a quite general open problem—the existence of 2D gap solitons with self-attractive intrinsic nonlinearity. This possibility could be numerically checked by gradually increasing V_0 starting from $V_0 = 0.324$. Figure 8 shows a 2D gap soliton supported by the self-attractive nonlinearity ($g = +1$) at $V_0 = 0.33$. Its existence is attributed to the fact that the amplitude or the norm of the imaginary part of the gap soliton is comparable to (or even larger than) that of the real part, in contrast to the case of the gap soliton with self-repulsive nonlinearity. This is also the reason why the profile of the current gap soliton is no longer quasi-isotropic, as can be seen from a comparison between Figs. 8(d) and 5(d). Furthermore, double peaks emerge in the real part as well as in the modulus. A valley also shows up in the real part, making it look like a dipole. These unique features are the direct and natural outcome of the $\mathcal{PT}$ potential. We verified that these

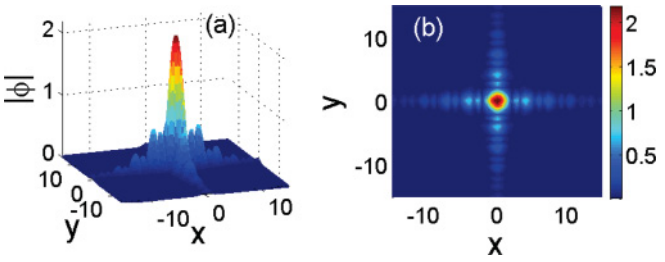

FIG. 6. (Color online) Similar to Fig. 5, but in the second band gap, for $V_0 = 0.02$, $g = -1$, $\mu = -2.43$, and $N = 4$. (a) is the mod of wave function $|\phi|$ and (b) is its contour plot.

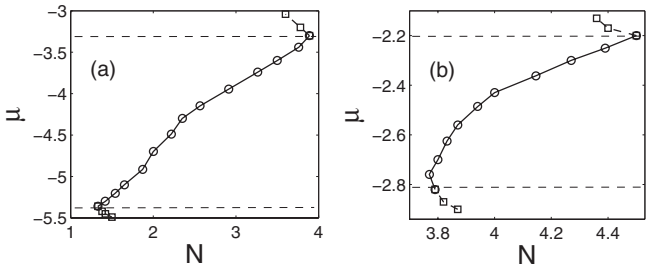

FIG. 7. The function $\mu(N)$ for the gap solitons in the (a) first and (b) second band gap with the 2D $\mathcal{PT}$ linear potential. The solid line represents the stable solitons (located inside the marked stripe), the dashed line corresponding to the unstable ones.

gap solitons always collapse in finite time (not shown here). Reconfirming the fact that both ordinary ones and gap solitons are stable only for small V_0, e.g., the instability appears when $V_0 \geqslant 0.04$, demonstrated by extensive numerical calculations. This is vastly different from the 1D case, where a soliton survives even for a moderate value of V_0, e.g., $V_0 = 0.45$ in Fig. 3 of Ref. [13].

V. LOCALIZED STATES IN THE LOW-DIMENSIONAL $\mathcal{PT}$ LINEAR LATTICE POTENTIAL

Another interesting issue is to create localized states in the low-dimensional $\mathcal{PT}$ potential. The profile of a localized state, produced in the Q1D potential, is highly stretched in the y direction, as displayed in Fig. 9, since the soliton is constrained by the Q1D potential only in one direction (i.e., the x axis). The bifurcation diagram of the 2D soliton in the Q1D potential is depicted in Fig. 3(b). Again agreeing with the VA criterion [24], the soliton family is stable when $\partial\mu/\partial N < 0$.

In addition, we demonstrated that the localized modes—both the ordinary and the gap solitons (whether in the first or

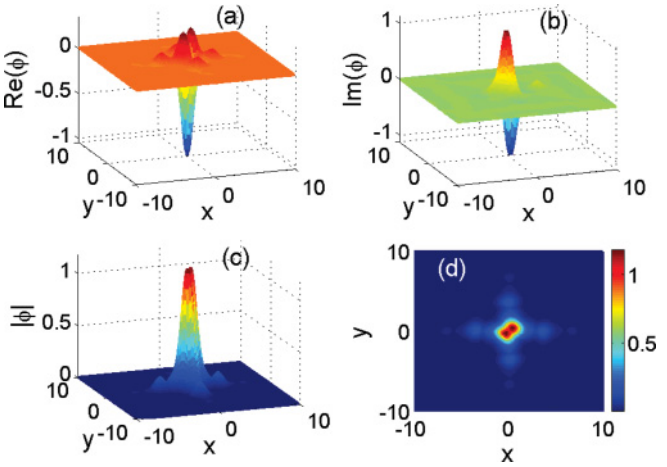

FIG. 8. (Color online) Similar to Fig. 5, but for the unstable gap soliton with self-attractive nonlinearity ($g = +1$), at $V_0 = 0.33$, $\mu = -3.8$, and $N = 2.1$. (a) and (b) are the real and imaginary parts of wave function $\phi(x,y)$, (c) is the mod of wave function $|\phi|$, and (d) is its contour plot.

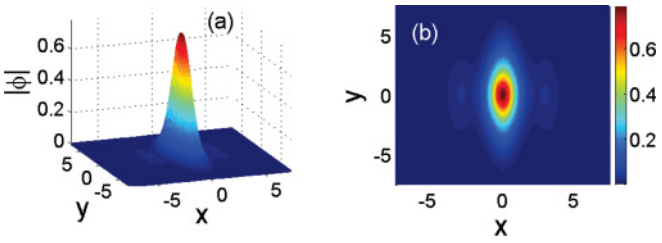

FIG. 9. (Color online) Similar to Fig. 2, but with the Q1D $\mathcal{PT}$ linear potential, for $V_0 = 0.02$, $g = +1$, $\mu = -2.925$, and $N = 0.91$. (a) is the mod of wave function $|\phi|$ and (b) is its contour plot.

second band gap), constructed for the imaginary Q1D $\mathcal{PT}$ potential [i.e., $V(x,y) = 4(\cos^2 x + \cos^2 y) + 4iV_0 \sin(2x)$]—are very similar to their full 2D counterparts (not shown here). This finding is very important because it may potentially simplify the fabrication of compact integrated $\mathcal{PT}$ photonic devices in the future. Furthermore, a decrease of the imaginary component in the Q1D potential will help curb the collapse of solitons to a certain extent.

VI. CONCLUSIONS

We studied the two-dimensional (2D) localized states, including both ordinary and gap solitons, in the 2D and the quasi-one-dimensional (Q1D) parity-time ($\mathcal{PT}$) linear lattice potentials. The stabilities of these solitons are examined with direct numerical simulation by adding small random perturbations (to both real and imaginary parts). A remarkable feature is that the imaginary part of the solitons always appears in the form of a dipole mode. The 2D gap solitons with self-attractive nonlinearity are found to exist as unstable states.

A challenging problem ensuing from this analysis is to stabilize the gap solitons with self-attractive nonlinearity [Fig. 8], i.e., to overcome or depress the smearing of the soliton with proper external interference. Furthermore, it could also be interesting to carry out a detailed analysis of solitons and solitary vortices by extending the current investigation to the hybrid system in the framework of combined linear and nonlinear $\mathcal{PT}$ lattices [21,25–28].

Note added. Recently, we learned that a similar work was published in Ref. [29], while where the 2D gap solitons have not been considered.

[1] C. M. Bender and S. Boettcher, Phys. Rev. Lett. **80**, 5243 (1998).
[2] S. Klaiman, U. Günther, and N. Moiseyev, Phys. Rev. Lett. **101**, 080402 (2008).
[3] A. Mostafazadeh, Phys. Rev. Lett. **102**, 220402 (2009).
[4] O. Bendix, R. Fleischmann, T. Kottos, and B. Shapiro, Phys. Rev. Lett. **103**, 030402 (2009).
[5] S. Longhi, Phys. Rev. Lett. **103**, 123601 (2009); **105**, 013903 (2010).
[6] Y. D. Chong, L. Ge, H. Cao, and A. D. Stone, Phys. Rev. Lett. **105**, 053901 (2010).
[7] Y. D. Chong, L. Ge, and A. D. Stone, Phys. Rev. Lett. **106**, 093902 (2011).
[8] W. Wan, Y. Chong, L. Ge, H. Noh, A. D. Stone, and H. Cao, Science **331**, 889 (2011).
[9] C. T. West, T. Kottos, and T. Prosen, Phys. Rev. Lett. **104**, 054102 (2010).
[10] A. E. Miroshnichenko, B. A. Malomed, and Y. S. Kivshar, Phys. Rev. A **84**, 012123 (2011).
[11] M. Liertzer, L. Ge, H. E. Türeci, and S. Rotterar, e-print arXiv:1109.0454v1.
[12] K. G. Makris, R. El-Ganainy, D. N. Christodoulides, and Z. H. Musslimani, Phys. Rev. Lett. **100**, 103904 (2008).
[13] Z. H. Musslimani, K. G. Makris, R. El-Ganainy, and D. N. Christodoulides, Phys. Rev. Lett. **100**, 030402 (2008).
[14] R. El-Ganainy, K. G. Makris, D. N. Christodoulides, and Z. H. Musslimani, Opt. Lett. **32**, 2632 (2007).
[15] D. N. Christodoulides and R. I. Joseph, Opt. Lett. **13**, 794 (1988).
[16] D. N. Christodoulides, F. Lederer, and Y. Silberberg, Nature (London) **424**, 817 (2003).
[17] A. Guo, G. J. Salamo, D. Duchesne, R. Morandotti, M. Volatier-Ravat, V. Aimez, G. A. Siviloglou, and D. N. Christodoulides, Phys. Rev. Lett. **103**, 093902 (2009).
[18] C. E. Ruter, K. G. Makris, R. El-Ganainy, D. N. Christodoulides, M. Segev, and D. Kip, Nature Phys. **6**, 192 (2010).
[19] K. G. Makris, R. El-Ganainy, D. N. Christodoulides, and Z. H. Musslimani, Phys. Rev. A. **81**, 063807 (2010); Int. J. Theor. Phys. **50**, 1019 (2011).
[20] M. C. Zheng, D. N. Christodoulides, R. Fleischmann, and T. Kottos, Phys. Rev. A. **82**, 010103(R) (2010).
[21] F. Kh. Abdullaev, Y. V. Kartashov, V. V. Konotop, and D. A. Zezyulin, Phys. Rev. A. **83**, 041805(R) (2011).
[22] S. V. Dmitriev, A. A. Sukhorukov, and Y. S. Kivshar, Opt. Lett. **35**, 2976 (2010).
[23] C. J. Pethick and H. Smith, *Bose-Einstein Condensate in Dilute Gas* (Cambridge University Press, Cambridge, 2008).
[24] M. Vakhitov and A. Kolokolov, Radiophys. Quantum. Electron. **16**, 783 (1973).
[25] H. Sakaguchi and B. A. Malomed, Phys. Rev. A **81**, 013624 (2010).
[26] J. Zeng and B. A. Malomed, Phys. Scr. (in press), e-print arXiv:1201.2254v1.
[27] J. Zeng and B. A. Malomed, Phys. Rev. A **85**, 023824 (2012).
[28] Y. V. Kartashov, B. A. Malomed, and L. Torner, Rev. Mod. Phys. **83**, 247 (2011).
[29] S. Nixon, L. Ge, and J. Yang, Phys. Rev. A **85**, 023822 (2012).